Deep Features Extraction for Endoscopic Image Matching

Houda Chaabouni-Chouayakh[1,2], Manel Farhat[1,2] and Achraf Ben-Hamadou[1,2]
[1]Centre de Recherche en Numérique de Sfax, 3021, Sfax, Tunisia
[2]Laboratory of Signals, Systems, Artificial Intelligence and Networks (SM@RT), Sfax, Tunisia

Keywords: Endoscopic Images,Deep Learning, Image Feature Matching, Adaptive Triplet Loss.

Abstract: Image feature matching is a key step in creating endoscopic mosaics of the bladder inner walls, which help urologists in lesion detection and patient follow-up. Endoscopic images, on the other hand, are particularly difficult to match because they are weekly textured and have limited surface area per frame. Deep learning techniques have recently gained popularity in a variety of computer vision tasks. The ability of convolutional neural networks (CNNs) to learn rich and optimal features contributes to the success of these methods. In this paper, we present a novel deep learning based approach for endoscopic image matching. Instead of standard handcrafted image descriptors, we designed a CNN to extract feature vector from local interest points. We propose an efficient approach to train our CNN without manually annotated data. We proposed an adaptive triplet loss which has the advantage of improving the inter-class separability as well as the inter class compactness. The training dataset is automatically constructed, each sample is a triplet of patches: an anchor, one positive sample (a perspective transformation of the anchor) and one negative sample. The obtained experimental results show at the end of the training step a more discriminative space representation where the anchor becomes closer to the positive sample and farther from the negative one in the embedding space. Comparison with the well-known standard hand-crafted descriptor SIFT in terms of recall and precision showed the effectiveness of the proposed approach, reaching the top recall value for a precision value of 0.97.

1 INTRODUCTION

Endoscopy is a widely used clinical procedure for the early detection of numerous cancers (*e.g.,* nasopharyngeal, oesophageal adenocarcinoma, gastric, colorectal cancers, bladder cancer, *etc.*) and therapeutic procedures (*e.g.,* polypectomy, injection sclerotherapy, variceal banding, *etc.*). An endoscope is the instrument used during an endoscopic exploration. It could be a rigid or flexible thin tube equipped by a lighting source and a camera. The doctor visualizes the captured stream of video endoscopy while exploring the inner surfaces of hollow organs.

Nevertheless, endoscopy has several limitations due mainly to the limited field of view and reduced maneuverability inside the bladder. Indeed, anomalies are usually spread over areas larger than the field of view making lesion partitions laid out over many frames in the endoscopic video. This makes organs exploration and anomalies detection time consuming and difficult for the doctors since they should follow the spatial distribution of the lesions over several frames. In addition, the ability to find structure similarities between images taken from different views or during different clinical examinations is a tough task. To address this issue, it is a common practice to replace the clinical endoscopic video with a panoramic image generated by stitching the video frames in a common coordinate system that covers a wide region of interest. For the generation of panoramic images, feature matching and finding correspondence between images is a key step.

Because of the large variability in texture and appearance aspect of the endoscopic images between patients, developing a robust and accurate feature matching between endoscopic images is particularly difficult. So far, this matching problem has been addressed by either directly computing classical similarity measures between the images (*e.g.,* mutual information, cross-correlation, *etc.*) or by using hand-crafted features such as SIFT(Lowe, 2004), SURF(Bay et al., 2008), *etc.* The main advantages of such algorithms are the simplicity and the efficiency. The basic idea in this case is to first extract features for a set detected image interest points. After that, point matching between images is per-

Chaabouni-Chouayakh, H., Farhat, M. and Ben-Hamadou, A.
Deep Features Extraction for Endoscopic Image Matching.
DOI: 10.5220/0010833700003124
In *Proceedings of the 17th International Joint Conference on Computer Vision, Imaging and Computer Graphics Theory and Applications (VISIGRAPP 2022) - Volume 4: VISAPP*, pages 925-932
ISBN: 978-989-758-555-5; ISSN: 2184-4321

formed based on the distance between their feature vectors. This category of techniques has previously been used to stitch images for various applications including remote sensing (Ait-Aoudia et al., 2012), underwater navigation (Elibol et al., 2017), retina analysis (Hossein-Nejad and Nasri, 2018), and endoscopy (Behrens et al., 2009; Bergen et al., 2013). In the case of endoscopic images, we can cite for instance the works of (Weibel et al., 2010; Ben-Hamadou et al., 2016; Daul et al., 2010; Behrens et al., 2010; Du et al., 2011). In particular, (Behrens et al., 2010) and (Du et al., 2011) propose respectively a SURF feature descriptor for real-time bladder mosaicing in fluorescence endoscopy and a SIFT-based descriptor for endoscopic zone matching. Recently, feature extraction from endoscopic images has been addressed in the work of (Martinez et al., 2020) where color and texture features are extracted and then exploited by classical classifiers such as a random forest tree or a KNN ensemble model for the classification of kidney stone captured with ureteroscopes. Later, the authors showed in (Lopez et al., 2021) how CNN-based solutions can further improve the classification of kidney stones, even when using a moderate number of images.

Nowadays, deep learning techniques clearly outperform standard and hand-crafted techniques for a wide range of computer vision tasks including face recognition (Lai et al., 2019), artifacts classification (Ali et al., 2021), image feature matching (Liu et al., 2018), denoising (Zou et al., 2019), classification (Kim et al., 2021; Liu et al., 2020), and segmentation (Ghosh et al., 2018). When it comes to endoscopy, to the best of our knowledge, no previous study has been proposed to build local features for endoscopic image matching based on deep learning techniques.

In this context, we propose in this paper a new deep learning-based method for learning local features to improve endoscopic image matching. We designed a CNN to transform local patches around image interest points instead of applying standard hand-crafted descriptors. The proposed training scheme of the CNN does not require manual annotation of data. We rather automatically construct a dataset of image patches triplets. Each triplet consists of an anchor patch, one positive patch (which is a perspective transformation of the anchor) and one negative patch. During the training process, the network parameters are trained with an adaptive triplet loss and updated so that for a given training triplet, the anchor-positive distance is minimized, while the anchor-negative distance is maximized. The learned CNN features are then used to classify the dataset and estimate the inter-class separability and intra-class compactness. A comparison with the classical SIFT descriptor is carried out in terms of precision/recall as in (Mikolajczyk and Schmid, 2005) to evaluate the efficiency of the learned CNN features.

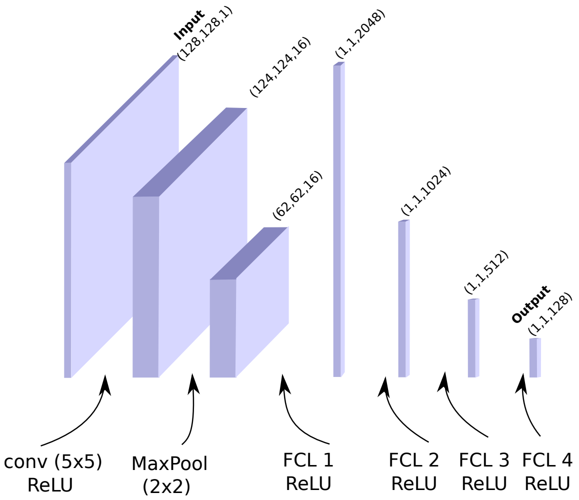

Figure 1: Proposed CNN architecture. For a given 128 × 128 patch, a 128-dimensional feature vector is provided in the embedding space.

The organization of this paper is as follows: Section 2 describes the proposed approach. Experimental results are presented and discussed in section 3. Finally, section 4 provides conclusions and future works.

2 PROPOSED APPROACH

This section details the proposed CNN architecture as well as training steps that lead to a discriminative feature space to describe all extracted patches around image interest points. The main idea consists then in training the proposed CNN with a set of patch triplets in order to optimize an adaptive triplet loss that encourages similar patches to be closer in the feature space. Comes after the feature matching step which is achieved via computation of Euclidean distances between features in the embedding space.

2.1 CNN Architecture

The CNN proposed in this work is applied on input patches of size 128 × 128. Figure 1 details the architecture of the proposed CNN. First, a 2D convolution followed by a ReLU activation layer is applied to the input data. Comes after a (2 × 2) max-pooling. After that, 4 Fully Connected Layers (FCLs) intercepted with ReLU activation layers are used. Finally, a normalization of the data has been carried on. This archi-

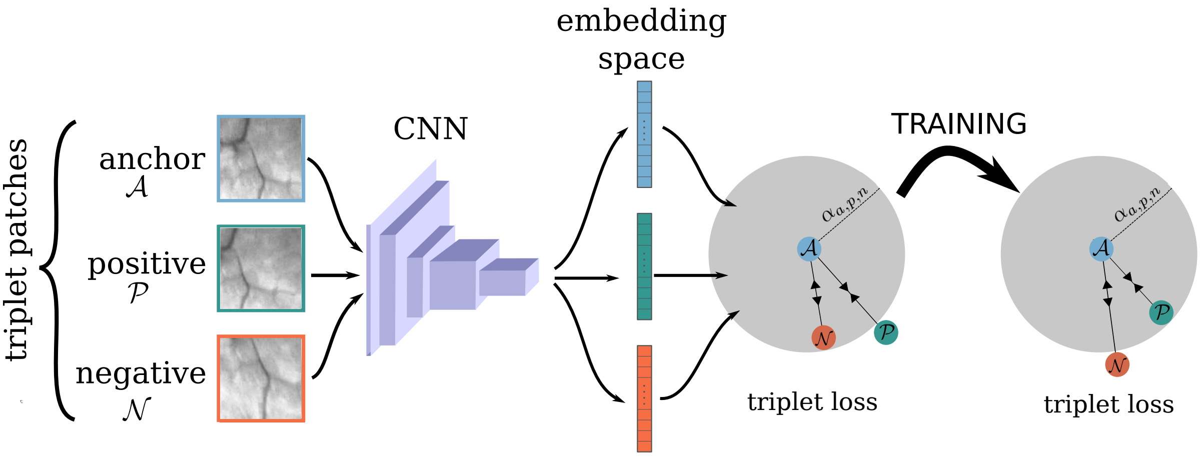

Figure 2: Triplet loss training approach. Features extracted from anchor, positive and negative samples are fed to the triplet loss and trained so that the anchor-positive distance is minimized and the anchor-negative one is maximized in the feature space. A more discriminative embedding space is thus obtained.

tecture provides at the end a 128- dimensional feature vector.

2.2 CNN Training

The generation of the training dataset is explained as follows: First, the raw data is converted from color to gray-scale images. The contrast of the images is then enhanced. After that, image interest points are detected without loss of generality via SIFT detector. Anchor patches are gathered by cropping 128 by 128 pixels around the detected image interest points. It is noticeable that organ surfaces are typically imaged from various angles and perspectives. In order to get the corresponding positive patches, we apply pseudo randomly generated perspective transformations on the set of collected anchor patches. In fact, such transformations could simulate well typical angles/perspective changes in endoscopic videos. The obtained positive patches have the advantage to appear very similar to anchor patches. The negative ones, on the other hand, are chosen randomly from the rest of the anchors and positive samples of other triplets. Figure 3 shows some examples of constructed patch triplets.

Depending on the desired prediction task, many loss functions have been proposed in the literature. In this work, we opted for the triplet loss to train our model. Triplet loss, introduced in (Schroff et al., 2015) as FaceNet model, has been successfully used in several tasks (Vygon and Mikhaylovskiy, 2021; Kumar et al., 2021). It has the advantage to enforce the inter-class separability as well as the intra-class compactness. The main idea consists in comparing a baseline (anchor) input to a positive (truthy) input and a negative (falsy) input. During the optimization process, the network parameters are updated so that the anchor-positive input distance is minimized, while the anchor-negative input distance is maximized. Figure 2 illustrates the complete principle of the adaptive triplet loss.

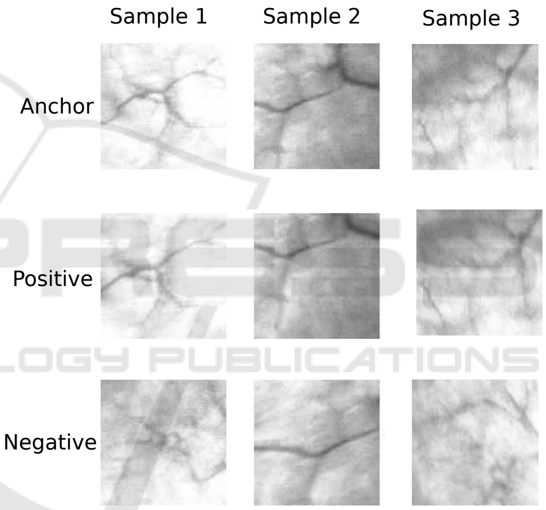

Figure 3: Three samples (*i.e.,* sample 1, 2 and 3) of collected triplet patches. An anchor is a patch cropped around an image interest point, already detected without loss of generality via SIFT detector. While the positive sample is a perspective transformation of the respective anchor, the negative one is chosen randomly from the rest of the anchors and positive samples of another triplet.

The triplet loss proposed in this work is defined by the following equation:

$$\mathcal{L} = \sum_{a,p,n \in \{A,P,N\}} \left(\|f(a) - f(p)\|_2^2 - \|f(a) - f(n)\|_2^2 + \alpha_{a,p} \right) \tag{1}$$

where $\{A, P, N\}$ denotes the triplets set: A, P and N are respectively the anchor, positive and negative inputs. $\|.\|_2$ is the Euclidean distance. The function $f(.)$ stands for the feature embedding function that maps a patch in the Euclidean embedding space via the CNN architecture illustrated in Figure 1. Minimizing $\mathcal{L}$ enforces the maximization of the Euclidean distance between patches from different classes (anchor and negative) which should be greater than the distance between anchor and positive features in the embedding space. In other words, the optimization process aims at updating the different network parameters so that the patches A and P become closer while A and N are further apart in the Euclidean embedding space.

The term $\alpha_{a,p}$ in Eq.(1) refers to a dynamic margin. It is designed as follows:

$$\alpha_{a,p} = \frac{\|f(a) - f(p)\|_2^2}{2}. \tag{2}$$

In this work, we have noticed experimentally that the use of adaptive margin is more advantageous than the fixed ones.

It is worth to note that adaptive margins have been used in many applications such as person reidentification (Li et al., 2018), image retrieval (Zhao et al., 2019). Promising results were obtained showing that adaptive triplet loss encourages the learned image embedding models to generalize well on cross-domain data.

2.3 Feature Matching

The step after feature extraction with the trained CNN is feature matching where the Euclidean distance between patches P_t and P_{t+1} cropped from two consecutive frames is computed in the embedding space according to the following equation:

$$D(f(P_{t+1}), f(P_t)) = \|f(P_{t+1}) - f(P_t)\|_2^2 \tag{3}$$

This definition transforms finding patch matching problem into a nearest neighbor search problem in the Euclidean space. In this work, we utilized Nearest Neighbor with a Threshold (NNT) to match patches in which matching pairs is identified if the distance is smaller than a certain threshold[1]. Note that, thresholding based matching is commonly used to evaluate descriptor performances (Lee and Park, 2014).

3 EXPERIMENTAL RESULTS AND DISCUSSIONS

We ran a series of experiments to evaluate the performance of the proposed endoscopic image matching in terms of True/False image interest point matching. We additionally compared the obtained results to SIFT descriptor, one of the well known state-of-the-art hand-crafted image descriptors.

3.1 Dataset Construction

To evaluate the proposed model, we collected a set of 300 image interest points from clinical patient endoscopic data with very different appearances. After that, positive and negative patches are constructed as already explained in 2. Figure 4 illustrates the dataset construction process.

3.2 CNN Training

When applying the CNN architecture proposed in this paper to the dataset described previously, the loss displayed in Figure 5 has been obtained, showing the convergence of the model. The data has been trained with a batch size of 36 using Stochastic Gradient Descent with an initial learning rate of 0.001 and a momentum set of 0.9. To avoid the over fitting of the model to the selected patch triplets, we update the training dataset each 50 epochs. The total number of epochs is 250. The total number of triplets is over 15000 triplets.

3.3 Obtained Results

The proposed model is evaluated in terms of:

- Discriminative ability of the obtained embedding space or in other words the representativeness of the generated features.
- Robustness to typical angles/perspective changes in endoscopic videos.

3.3.1 Discriminative Ability of the Embedding Space

In order to measure the ability of the proposed method to generate a discriminative embedding space representation of the dataset, we define three types of triplets; hard, semi-hard, and easy samples. The degree of easiness/ hardness is expressed in terms of inter-class separability and intra-class compactness. More Details about the different sample types are given bellow:

[1] In our case, we set experimentally the NNT threshold to 5.

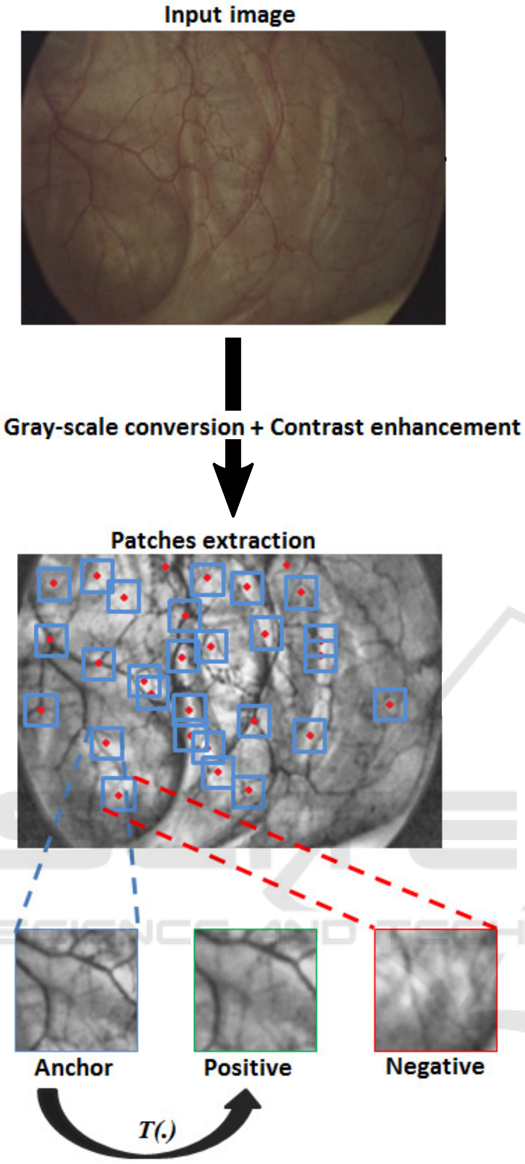

Figure 4: After conversion to gray-scale level and contrast enhancement, image interest points are detected. Anchors are obtained by cropping 128 by 128 pixels around the detected image interest points. While positive patches are perspective transformation of the corresponding anchors (via $T(.)$), the negative ones are selected randomly from the rest of anchors and positives.

- **Hard Samples:** in this case, the samples will be matched as false positives since the anchor-positive distance is greater than the anchor-negative one.

$$\|f(a)-f(p)\|_2^2 > \|f(a)-f(n)\|_2^2$$

- **Semi-hard Samples:** in this case, the anchor-positive distance is still smaller than the anchor-negative one but becomes larger when adding the adaptive margin. Formally:

$$\|f(a)-f(p)\|_2^2+\alpha_{a,p} > \|f(a)-f(n)\|_2^2.$$

- **Easy Samples:** these samples should also be called safe samples. In here, it is easy to separate the negative patch. In face, these samples are characterized by the fact that the anchor-positive distance remains always smaller than the anchor-negative one even when adding the adaptive margin. Mathematically speaking:

$$\|f(a)-f(p)\|_2^2+\alpha_{a,p} < \|f(a)-f(n)\|_2^2.$$

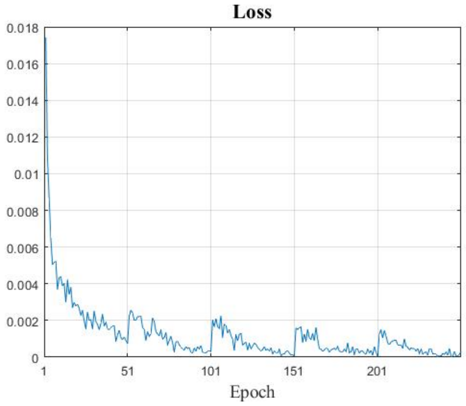

Figure 5: Convergence of the loss of the proposed approach. An update of the training dataset is carried on every 50 epochs to avoid the over fitting. We notice that the loss increases systematically on each dataset update but starts again to decrease.

From the definitions given above, it is clear that the larger the proportion of easy samples is, the more discriminative the embedding space is, and the respectively the larger the proportion of the hard samples is, the less discriminative the embedding space is.

During the training process we monitor the proportion (or percentage) of each of the three triplet types. The idea is to check if during the training the obtained feature space allows to increase the proportion of easy samples at the expense of semi-hard and hard samples, resulting thus in a more discriminative feature space. Figure 6 summarizes the updates of the easy-to-hard partition of the triplet samples during the training step.

As depicted in Figure 6, we could notice that the semi-hard samples proportion decreases dramatically, while the easy samples one gets higher, reaching more than 90% at the end of the training process. This means that through the optimization process, the different network parameters are updated so that the learned features transfer samples from the hard, semi-hard packages to the easy one, where the matching between the anchor and positive patches becomes more intuitive.

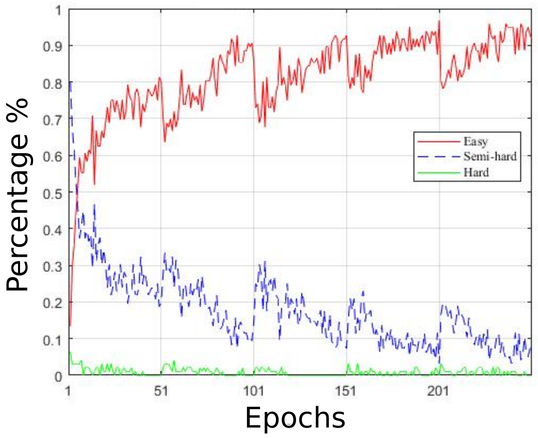

Figure 6: Easy-to-hard partition of the triplet samples. We observe that over training epochs a more discriminative space representation is estimated allowing the an easy separation between positive and negative samples. The proportion of easy samples increases (reaching more than 90%) at the expense of semi-hard and hard samples (together less than 10%).

3.3.2 Robustness of the Model to Viewpoint Changes

When using an endoscope, organ surfaces are typically imaged from various angles and perspectives, resulting in a stream of video endoscopy. Therefore, we evaluate the performance of our approach in matching interest points in the same endoscopic video in terms of robustness against viewpoint changes. We also compare it to the well-known standard hand-crafted descriptor SIFT.

To simulate typical viewpoint changes in endoscopic videos, we first detect image interest points and then estimate homographies from real clinical data between consecutive frames based on RANSAC algorithm (Fischler and Bolles, 1981).

Ten sequences of human bladder endoscopic videos from different patients have been used for this purpose. Each sequence consists of thousands of frames with a wide range of texture, luminosity, and appearance. Homologous points matching between consecutive frames has been manually performed to collect the matching ground truth. Once homographies have been estimated, we randomly apply them to image sequences. For each pair of images (*i.e.,* original and warped images), image interest points are detected. Then, point matching is performed twice, using our method and SIFT method. Evaluation is carried out qualitatively and quantitatively to compare the two methods.

Figure 7 depicts the qualitative evaluation of the SIFT descriptor and the proposed one when matching two endoscopic frames. Green and red lines refer respectively to correct and wrong matches. Compared to SIFT, we can observe that a larger number of correct matches (green lines) is achieved with our approach.

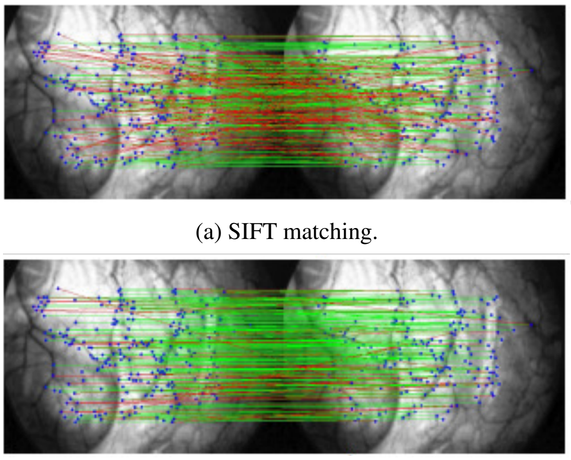

(a) SIFT matching.

(b) Our matching.

Figure 7: Qualitative evaluation of the matching performances carried out between two endoscopic frames. Image interest points are colored in blue. Green and red lines refer respectively to correct and wrong matches. The best matching quality is reached with our approach.

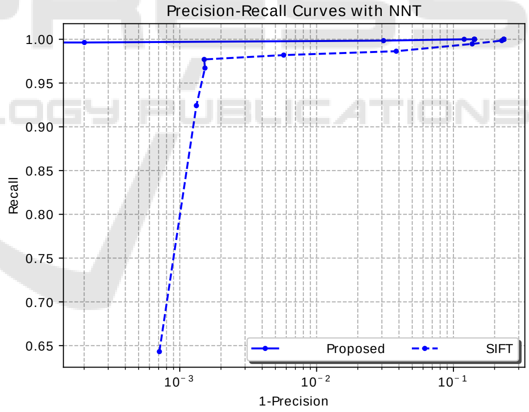

Figure 8: Quantitative evaluation: Recall/precision computed for SIFT and proposed approach when varying viewpoint angles. The proposed descriptor outperforms SIFT, reaching the maximal recall value for a precision value of 0.97.

For quantitative evaluation, we compare our learned features matching performance to the SIFT one in terms of *recall* with regard to *precision*. The obtained results are depicted in Figure 8. We can see that our method outperforms SIFT reaching the top recall value for a precision value of 0.97. Another advantage of the method over hand-crafted approaches such as SIFT is that the proposed training scheme does not require manual annotation, allowing for additional few steps of fine tuning without manual intervention for a better adaptation of the CNN model for the sequence specificity without loss of generality of the approach.

4 CONCLUSIONS AND FUTURE WORKS

In this work, we propose the first deep learning based approach for endoscopic image matching. For this purpose, a triplet-based dataset of image patches triplet has been firstly constructed. After that, to train the CNN, an adaptive triplet loss has been designed to improve the inter-class separability as well as the inter class compactness leading to a discriminative feature space. We assessed the robustness of the proposed approach against viewpoint changes and compared the obtained performances to SIFT, one of the most successful state-of-art descriptors.

Our further work will be focused on exploring graph neural networks to integrate neighboring image interest points in order to improve the discriminative ability of the model. We intend also to test our approach on other endoscopic data captured for different organs.

REFERENCES

Ait-Aoudia, S., Mahiou, R., Djebli, H., and Guerrout, E.-H. (2012). Satellite and Aerial Image Mosaicing - A Comparative Insight. In *2012 16th International Conference on Information Visualisation*, pages 652–657, Montpellier, France. IEEE.

Ali, S., Zhou, F., Bailey, A., Braden, B., East, J. E., Lu, X., and Rittscher, J. (2021). A deep learning framework for quality assessment and restoration in video endoscopy. *Medical Image Analysis*, 68:101900. Publisher: Elsevier.

Bay, H., Ess, A., Tuytelaars, T., and Van Gool, L. (2008). Speeded-Up Robust Features (SURF). *Computer Vision and Image Understanding*, 110(3):346–359.

Behrens, A., Bommes, M., Stehle, T., Gross, S., Leonhardt, S., and Aach, T. (2010). Real-time image composition of bladder mosaics in fluorescence endoscopy. *Computer Science - Research and Development*.

Behrens, A., Stehle, T., Gross, S., and Aach, T. (2009). Local and global panoramic imaging for fluorescence bladder endoscopy. In *2009 Annual International Conference of the IEEE Engineering in Medicine and Biology Society*, pages 6990–6993. IEEE.

Ben-Hamadou, A., Daul, C., and Soussen, C. (2016). Construction of extended 3d field of views of the internal bladder wall surface: A proof of concept. *3D Research*, 7(3):1–23.

Bergen, T., Wittenberg, T., Münzenmayer, C., Chen, C. C. G., and Hager, G. D. (2013). A graph-based approach for local and global panorama imaging in cystoscopy. In *Medical Imaging 2013: Image-Guided Procedures, Robotic Interventions, and Modeling*, volume 8671, page 86711K. International Society for Optics and Photonics.

Daul, C., Blondel, W., Ben-Hamadou, A., Miranda-Luna, R., Soussen, C., Wolf, D., and Guillemin, F. (2010). From 2d towards 3d cartography of hollow organs. In *2010 7th International Conference on Electrical Engineering Computing Science and Automatic Control*, pages 285–293. IEEE.

Du, P., Zhou, Y., Xing, Q., and Hu, X. (2011). Improved SIFT matching algorithm for 3D reconstruction from endoscopic images. In *Proceedings of the 10th International Conference on Virtual Reality Continuum and Its Applications in Industry*, pages 561–564.

Elibol, A., Kim, J., Gracias, N., and Garcia, R. (2017). Fast Underwater Image Mosaicing through Submapping. *Journal of Intelligent & Robotic Systems*, 85(1):167–187.

Fischler, M. A. and Bolles, R. C. (1981). Random sample consensus: a paradigm for model fitting with applications to image analysis and automated cartography. *Communications of the ACM*, 24(6):381–395. Publisher: ACM New York, NY, USA.

Ghosh, T., Li, L., and Chakareski, J. (2018). Effective deep learning for semantic segmentation based bleeding zone detection in capsule endoscopy images. In *2018 25th IEEE International Conference on Image Processing (ICIP)*, pages 3034–3038. IEEE.

Hossein-Nejad, Z. and Nasri, M. (2018). A-RANSAC: Adaptive random sample consensus method in multimodal retinal image registration. *Biomedical Signal Processing and Control*, 45:325–338. Publisher: Elsevier.

Kim, Y. J., Bae, J. P., Chung, J.-W., Park, D. K., Kim, K. G., and Kim, Y. J. (2021). New polyp image classification technique using transfer learning of network-in-network structure in endoscopic images. *Scientific Reports*, 11(1):1–8. Publisher: Nature Publishing Group.

Kumar, P., Jain, S., Raman, B., Roy, P. P., and Iwamura, M. (2021). End-to-end Triplet Loss based Emotion Embedding System for Speech Emotion Recognition. In *2020 25th International Conference on Pattern Recognition (ICPR)*, pages 8766–8773. IEEE.

Lai, S.-C., Kong, M., Lam, K.-M., and Li, D. (2019). High-resolution face recognition via deep pore-feature matching. In *2019 IEEE International Conference on Image Processing (ICIP)*, pages 3477–3481. IEEE.

Lee, M. H. and Park, I. K. (2014). Performance evaluation of local descriptors for affine invariant region detector. In *Asian Conference on Computer Vision*, pages 630–643. Springer.

Li, Z., Sang, N., Chen, K., Gao, C., and Wang, R. (2018). Learning deep features with adaptive triplet loss for person reidentification. In *MIPPR 2017: Pattern*

Recognition and Computer Vision, volume 10609, page 106090G. International Society for Optics and Photonics.

Liu, G., Hua, J., Wu, Z., Meng, T., Sun, M., Huang, P., He, X., Sun, W., Li, X., and Chen, Y. (2020). Automatic classification of esophageal lesions in endoscopic images using a convolutional neural network. *Annals of translational medicine*, 8(7). Publisher: AME Publications.

Liu, Y., Xu, X., and Li, F. (2018). Image feature matching based on deep learning. In *2018 IEEE 4th International Conference on Computer and Communications (ICCC)*, pages 1752–1756. IEEE.

Lopez, F., Varela, A., Hinojosa, O., Mendez, M., Trinh, D.-H., ElBeze, J., Hubert, J., Estrade, V., Gonzalez, M., Ochoa, G., and Daul, C. (2021). Assessing deep learning methods for the identification of kidney stones in endoscopic images. *arXiv:2103.01146 [cs, eess]*. arXiv: 2103.01146.

Lowe, D. G. (2004). Distinctive image features from scale-invariant keypoints. *International journal of computer vision*, 60(2):91–110. Publisher: Springer.

Martinez, A., Trinh, D.-H., El Beze, J., Hubert, J., Eschwege, P., Estrade, V., Aguilar, L., Daul, C., and Ochoa, G. (2020). Towards an automated classification method for ureteroscopic kidney stone images using ensemble learning. In *2020 42nd Annual International Conference of the IEEE Engineering in Medicine & Biology Society (EMBC)*, pages 1936–1939, Montreal, QC, Canada. IEEE.

Mikolajczyk, K. and Schmid, C. (2005). A performance evaluation of local descriptors. *IEEE Transactions on Pattern Analysis and Machine Intelligence*, 27(10):1615–1630. Conference Name: IEEE Transactions on Pattern Analysis and Machine Intelligence.

Schroff, F., Kalenichenko, D., and Philbin, J. (2015). Facenet: A unified embedding for face recognition and clustering. In *Proceedings of the IEEE conference on computer vision and pattern recognition*, pages 815–823.

Vygon, R. and Mikhaylovskiy, N. (2021). Learning Efficient Representations for Keyword Spotting with Triplet Loss. *arXiv preprint arXiv:2101.04792*.

Weibel, T., Daul, C., Wolf, D., Rösch, R., and Ben-Hamadou, A. (2010). Endoscopic bladder image registration using sparse graph cuts. In *2010 IEEE International Conference on Image Processing*, pages 157–160. IEEE.

Zhao, X., Qi, H., Luo, R., and Davis, L. (2019). A weakly supervised adaptive triplet loss for deep metric learning. In *Proceedings of the IEEE/CVF International Conference on Computer Vision Workshops*, pages 0–0.

Zou, S., Long, M., Wang, X., Xie, X., Li, G., and Wang, Z. (2019). A CNN-Based Blind Denoising Method for Endoscopic Images. In *2019 IEEE Biomedical Circuits and Systems Conference (BioCAS)*, pages 1–4. IEEE.